Selected Papers of The Society of Naval Architects of Korea, Vol. 1, 1993. pp. 15~25.

A Potential-Based Panel Method for the Analysis of a Two-Dimensional Partially-Cavitating Hydrofoil

Chang – Sup Lee*

(From T.S.N.A.K., Vol.26, No.4, 1989)

Abstract

A potential-based panel method is presented for the analysis of a partially-cavitating two-dimensional hydrofoil. The method employs normal dipoles and sources distributed on the foil and cavity surfaces. It is shown that the source plays an important role in positioning the cavity surface through an iterative process. The cavity closure consition is found very effective in generating the cavity shape. Upon convergence, the method predicts the cavitation numer, together with the lift, the drag and the surface pressure distribution, for a given cavity length. Systematic convergence tests shows that the present numerical method is fast and stable. The present computations show a good agreement with the previously computed and measured results.

1. Introduction

As the loading on blades of a marine propeller increases, cavitation plays an important role in the unsteady hull forces and also causes severe noise and vibration problems at the stern. In order to control these problems at the stern of a ship and also to design a propeller with a sufficient but not excessive cavitation margin, it is desirable to predict the extent and behavior of the cavity on the surface of the propeller blades with an improved accuracy.

Traditional methods predicting the cavitation phenomenon around a marine propeller are based mostly on the linearized lifting surface theory (see, for example, Lee[1]). Upon linearization, the flow around the leading edge of a blade results in a singular pressure peak, which becomes inevitably the source of inaccurate overprediction of the cavity extent on the blades of a marine propeller. To overcome this drawback of the lifting-surface theory, a surface panel method is now emerging where the singularities such as sources and normal dipoles are distributed on the true blade surface rather than on the mean -line surface(Lee[2], Yang & Jessup [3], Hess & Valarezo [4]). The pressure distribution near the leading edge may now be predicted fairly accurately, and hence a reliable cavity prediction is foreseeable in the near future.

* Member, Chungnam National University

The aim of this paper, with an ultimate goal of application to marine propellers, is to develop a technique to solve the problems of partially-cavitating flows around two-dimensional hydrofoils of various profiles. Both the linear and nonlinear theories to solve the cavity flow around a two-dimensional section have been successful. A good review on the publications has recently been reported by Uhlman [5]. Due to its flexibility to deal with complicated blade geometry, the surface singularity distribution method draws a more attention nowadays. Recently Uhlman [5] solved the cavity flow problem by a boundary-integral method where he distributed the vorticities on the foil and cavity surfaces. Uhlman's nonlinear theory could predict various quantities of interest in cavity flow very successfully. One disadvantage in his theory is that the velocity-based formulation requires a large number of elements and also a large number of iterations to reach to the converged values, which is not favorable in three dimensional extensions.

The present theory is also a boundary-integral method, but employs the sources and normal dipoles to represent the foil and cavity surfaces.

The formulation takes the velocity potential as the basic unknown function, unlike the velocity-based formulation of Uhlman, and therefore the present theory is one order less singular than Uhlman's. It may therefore be expected that the number of minimum required elements and iterations for reasonable solutions would be less in the present method compared with Uhlman's.

This paper describes the boundary-value problem around a cavitating hydrofoil and the numerical method together with the results of extensive convergence tests. Comparisons of the numerical results with other theories and experiments are also shown here.

2. Statement of boundary-value problem

Let us consider the steady, irrotational flow of an inviscid, incompressible unbounded fluid past a two-dimensional cavitating hydrofoil. A Cartesian coordinate system is chosen as shown in Fig. 1 with the leading edge of the foil at the origin and the trailing edge on the positive x-axis. The uniform oncoming flow is inclined by an angle of attack α. The total velocity, $\underline{V}$, may be expressed in terms of the total velocity potential, Φ, which is defined using the oncoming velocity, $\underline{U}_\infty$, the position vector, $\underline{x}$, and the perturbation potential, ϕ, as follows :

$$\underline{V}=\nabla\Phi \tag{1}$$

where

$$\Phi=\underline{U}_\infty\cdot\underline{x}+\phi \tag{2}$$

The conservation of mass applied to the potential flow gives the Laplace equation as a governing equation, that is,

$$\nabla^2\Phi=0, \qquad \textit{throughout the fluid} \tag{3}$$

The flow can be uniquely defined by imposing the boundary condition on the boundary surfaces as follows :

1. Quiescence condition at infinity :

$$\nabla\Phi\rightarrow\underline{U}_\infty, \qquad \text{at infinity} \tag{4}$$

2. Flow tangency condition on the body surface:

$$\hat{n}\cdot\underline{V}=\frac{\partial\Phi}{\partial n}=0, \qquad \text{on the body surface } S_B \tag{5}$$

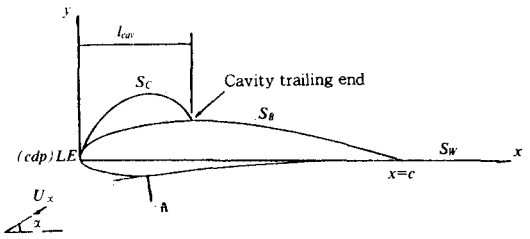

Fig. 1 Definition sketch of a cavitating hydrofoil

where $\hat{n}$ is the unit vector normal to the boundary, defined positive when pointing into the fluid region.

3. Kutta condition .

$$|\underline{V}_{T.E.}|<\infty, \quad \text{at the trailing edge} \tag{6}$$

where *T.E.* stands for the trailing edge.

For the partially-cavitating flow, the Kutta condition requires that the magnitude of the velocity is finite at the trailing edge as in the subcavitating flow.

With the presence of cavity on the hydrofoil, we have to apply the kinematic and dynamic boundary conditions on the cavity surface, the cavity closure condition at the cavity trailing end, and the cavity detachment condition.

4. Kinematic condition on the cavity surface :

$$\frac{DF}{Dt}=0, \quad \text{on the cavity surface } S_c \tag{7}$$

where $F(x,y)$ is a function expressing the cavity surface.

5. Dynamic condition on the cavity surface :

$$p=p_v, \quad \text{on the cavity surface } S_c \tag{8}$$

where p_v is the vapor pressure inside the cavity.

6. Cavity closure condition :

$$T^c(x_{cte})=0, \quad \text{at the cavity trailing end} \tag{9}$$

where $T^c(x)$ denotes the cavity thickness function and x_{cte} denotes the x-coordinate of the cavity trailing end.

According to Wu [6][7], the condition on which the cavity departs from the solid body surface is either fixed or free, depending on whether the point that the cavity flow detaches from the body (a) at a fixed point as in the trailing edge and the sharp leading edge, or (b) at some points on a smooth body, which is not known a priori, as for example in the case of flow around a thick round leading edge. The Wu's nonlinear theory states that the curvature of the streamline at the junction point of the body and cavity surfaces should be either infinite or finite for the fixed or free detachment points, respectively.

The detachment point at the leading edge of the thick hydrofoil section is not known in advance. The exact location is in fact governed by the real fluid effect, which is beyond the scope of the present study. We assumed here, to simplify the analysis, that the cavity starts from the leading edge of the foil, leaving the sensitivity of this assumption to be studied in the future. The cavity detachment at the sharp corner is really fixed and causes no ambiguity at the sharp leading edge.

Using the Bernoulli equation, we get relations between the surface pressure, p, the tangential speed on the foil-cavity surface, $|V_c|$, the cavitation number, σ, and the pressure coefficient, C_p, as follows :

$$C_p\equiv\frac{p-p_\infty}{\frac{1}{2}\rho U_\infty^2}=1-\left(\frac{|\underline{V}_c|}{U_\infty}\right)^2, \quad \text{on foil /cavity surface} \tag{10}$$

$$\sigma\equiv\frac{p_\infty-p_v}{\frac{1}{2}\rho U_\infty^2}=-C_{pv}=\left(\frac{|\underline{V}_c|}{U_\infty}\right)^2-1, \quad \text{on the cavity surface} \tag{11}$$

where $\underline{U}_\infty=|\underline{U}_\infty|$, ρ is the density of water, p_∞ is the ambient pressure and $|\underline{V}_c|$ is the tangential speed on the cavity surface.

According to (10) and (11), the dynamic condition on the cavity surface (8) can be replaced by the kinematic condition so that the tangential speed on the cavity surface, $|\underline{V}_c|$ is constant, that is

$$|\underline{V}_c|=const. \tag{12}$$

In this paper, we are interested in the lift, L, the drag, D, and the moment, M, acting on the hydrofoil in cavitating condition and also the cavity volume, Vol (or, the cavity section area in the present two-dimensional problem). The non-dimensional coefficients of these quantities are defined following the expression of Uhlman [5].

The lift coefficient, C_L, is given as

$$C_L \equiv \frac{L}{\frac{1}{2}\rho U_\infty^2 c} = -\oint_{S_B} C_p \hat{t} \cdot \frac{\underline{U}_\infty}{U_\infty} ds \tag{13}$$

the drag coefficient, C_D, is

$$C_D \equiv \frac{D}{\frac{1}{2}\rho U_\infty^2 c} = -\oint_{S_B} C_p \hat{n} \cdot \frac{\underline{U}_\infty}{U_\infty} ds \tag{14}$$

and the moment coefficient, C_M, about the origin (that is, the leading edge of the hydrofoil), is

$$C_M \equiv \frac{M}{\frac{1}{2}\rho U_\infty^2 c} = -\oint_{S_B} C_p \underline{\gamma} \times \hat{n}\, ds \tag{15}$$

where c denotes the chordlength and $\underline{\gamma}$ denotes a vector from the origin to a point on the foil surface ; $\hat{t}$ is the unit tangential vector defined in the clockwise direction along the foil surface as shown in Fig. 1.

The cavity volume, Vol, is calculated from the cavity thickness function, $T^c(x)$, as

$$Vol = \int_{x_l}^{x_{te}} T^c(x)\, dx \tag{16}$$

where l_{cav} is the cavity length defined along the x-axis as shown in Fig. 1.

3. Singularity distribution method

From Green's theorem, we may derive an expression for the potential in the flow field by distributing the normal dipoles and sources on the body surface, or alternatively by distributing only either the normal dipoles or sources as shown by Lamb[8]. From the literature (see, for example, Moran[9]), the lifting airfoil problem can be treated successfully by adopting only the normal dipoles on the foil surface and on the wake sheet. However, in the present cavity flow problem in addition to the normal dipoles, we introduce the sources to represent the presence of the cavity on the cavitating portion of the foil. We expect that the sources will serve as a normal flux generator, which may be integrated in the streamwise direction to form the cavity shape, in a similar manner as in the thickness problem of the thin wing theory.

The total potential in the fluid region may now be expressed as follows :

$$\begin{aligned}\Phi(\underline{x}) = \underline{U}_\infty \cdot x &+ \int_{S_B+S_C} \frac{\mu(\xi)}{2\pi} \frac{\partial}{\partial n_\xi} \log R(\underline{x};\underline{\xi})\, dS \\ &+ \int_{S_C} \frac{q(\xi)}{2\pi} \log R(\underline{x};\underline{\xi})\, dS \\ &+ \int_{S_W} \frac{\mu_w}{2\pi} \frac{\partial}{\partial n_\xi} \log R(\underline{x};\underline{\xi})\, dS\end{aligned} \tag{17}$$

where

$q(\xi)$ =source strength
$\mu(\xi)$ =dipole strength
$\underline{x}(x,y,z)$ =field point where induced potentials are calculated
$\xi(\xi,\eta,\zeta)$ =point where singularities are located
$R(\underline{x};\underline{\xi})$ =distance between points $\underline{x}$ and $\underline{\xi}$

$$= \sqrt{(x-\xi)^2+(y-\eta)^2+(z-\zeta)^2}$$

$\frac{\partial}{\partial \eta_\xi}$ =normal derivative with respect to point $\underline{\xi}$

and also S_B, S_C and S_W denote the body surface, the cavity surface and the wake sheet surface, respectively, and μ_w denotes the dipole strength on the wake sheet surface, S_W, which is negative of the jump of potentials across the wake sheet surface. The direction of the dipole in the wake sheet surface, S_W, is defined positive when pointing upward.

For dipole-only distribution, we may convert the flow tangency condition (5), $\partial\Phi/\partial n=0$, in the fluid side of the boundary into the zero total potential condition, for the fictitious internal flow, defined in Equation.

$$\Phi^{-}(\underline{x})=0 \tag{18}$$

where the superscript denotes that the velocity potential is to be calculated on the interior to the foil surface (see, for example, Breslin et al[10]). If we apply this conversion across the dipole and source sheet, we will inevitably introduce errors in the flow tangency boundary condition or nonzero normal flux due to the influence of the sources. Indeed, this normal flux on the current dipole and source sheet is in essence the thickness correction function necessary in searching the cavity shape. If this error term vanishes through iterations, due to the vanishing source strengths, the kinematic condition on the cavity surface will then be satisfied by the alternative form of the kinematic boundary condition for the internal flow defined in Equation(18).

Equation (17) may now be reformed and applied to a point on and inside the foil-cavity surface to meet the alternative form of the kinematic boundary condition (18) as

$$\begin{aligned}\Phi^{-}(\underline{x}=0=\underline{U}_{\infty}\cdot\underline{x}+\frac{\mu(\underline{x})}{2}&\\ +\int_{S_B\cup S_C}\frac{\mu(\xi)}{2\pi}\frac{\partial}{\partial n_\xi}\log R(\underline{x};\xi)\,dS&\\ +\int_{S_C}\frac{q(\xi)}{2\pi}\log R(\underline{x};\xi)\,dS&\\ +\int_{S_W}\frac{\mu_w}{2\pi}\frac{\partial}{\partial n_\xi}\log R(\underline{x};\xi)\,dS&\end{aligned} \tag{19}$$

The dipole in the wake, μ_w, is the negative of the potential jump at the trailing edge. For a steady lifting flow, the negative of μ_w is equivalent to the circulation around the hydrofoil and constant along the wake surface, S_w.

The Kutta condition (6) is replaced by Morino's[11] condition for the present potential-based method as

$$\mu_W=-(\Delta\Phi)_w \tag{20}$$

where $(\Delta\Phi)_w$ is the potential jump across the wake sheet surface, S_w, which extends to downstream infinity from the trailing edge. Due to the characteristics of singularities, the governing equation (3), and the quiescence condition (4), will automatically be satisfied. Since $\underline{U}_\infty\cdot\underline{x}$ in (19) is known, the equation (19) becomes an integral equation for the unknown strengths of source and normal dipole distributions.

Equation (12), derived from the dynamic boundary condition on the cavity surface, implies that the velocity potential on the cavity surface has a linearity, so that we can set

$$\Phi^{u}=\Phi^{u}_{cdp}+|\underline{V}_c|\int_0^{l_g}dS \tag{21}$$

where the superscript, u, represents the upper surface of the cavity, and the subscript cdp denotes the cavity detachment point and l_g denotes the girth length along the cavity surface from the cavity detachment point to the point where the potential is calculated. Thus, Φ^u denotes the velocity potentials on the upper surface of the cavity. Φ^u_{cdp} becomes the velocity potentials at the upper cavity detachment point near the leading edge. For the partially-cavitating flow with positive angle of attack, only the velocity potentials on the upper surface of the cavity, Φ^u and Φ^u_{cdp}, are considered.

Equation (21) relates the tangential speed on the cavity surface to the velocity potential, which is really a useful form, since the constant speed on the cavity surface $|\underline{V}_c|$ is linearly related to the unknown variables Φ or μ.

The source strength representing the thickness of the cavity or, more correctly, the function to relocate the current cavity surface position in an iterative process may be related, in a linearized sense, to the product of the oncoming velocity

and the first derivative of cavity thickness correction function, t^c as in the case of thin wing theory :

$$q = V_n = U_\infty \frac{dt^c}{dx} \tag{22}$$

$$t^c = T^c_{(i)} - T^c_{(i-1)} \tag{23}$$

where V_n is the normal component of the total velocity on the cavity surface, which is expected to be nonzero when the tangency boundary condition (5) is replaced by the zero total potential condition (18), and the subscript (i) denotes the iteration index. Equation (23) shows that t^c is the difference of the cavity surfaces between two successive iterations. Note that the source strength, $q(\xi)$, vanishes upon convergence.

Since the cavity thickness T is to satisfy the closure condition (9), the thickness correction function t^c should also satisfy the same condition. Integrating (22), we get expressions for the cavity thickness correction and an alternative form of the cavity closure condition as follows :

$$t^c(1) = \int_0^1 \frac{q}{U_\infty} dx \tag{24}$$

$$t^c(l_{cav}) = \int_0^{cav} \frac{q}{U_\infty} dx \tag{25}$$

Once equation (19) is solved, the cavity source strengths, $q(\xi)$, are known, and hence the new cavity shape may be obtained by correcting the ordinate of the cavity surface at the current iteration, as schematically shown in Fig. 2.

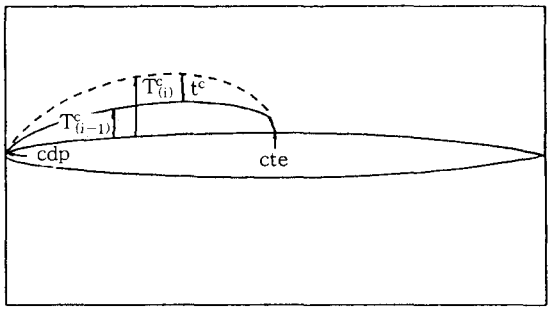

Fig. 2 Definition sketch of cavity surface position at each iteration

4. Numerical implementation of the problem

4.1 Discrete representation of hydrofoil and cavity surfaces

For numerical computation, the foil and cavity surfaces are replaced by a set of straight-line segments of finite length as shown in Fig. 3. The flow near the leading edge varies more rapidly than any other region around the foil, and hence the surface panel size should be smaller in this region. We adopted, to represent the x-coordinate of the panel boundary x^B as follows :

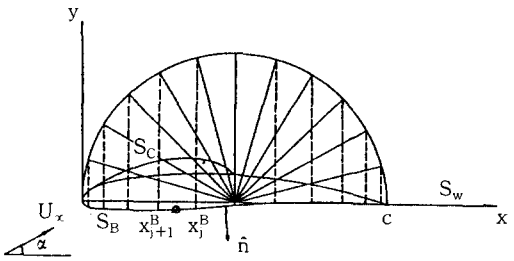

Fig. 3 Discretization of foil and cavity surfaces

$$x^B = \frac{c}{2}(1 - cos\theta),\ 0 \le \theta \le \pi \tag{26}$$

where the lower and upper limits of θ corresponds to the leading edge and trailing edge, respectively.

The x-coordinate of the cavity, x^C, is the same as the coordinate of the panel boundary above the upper surface of the foil, that is, $x^C = x^B$. The vertical coordinate of the hydrofoil, y^B, is computed by using the offset of the hydrofoil section, and that of the cavity, y^C, is obtained as a part of the solution. Fig. 3 shows the typical discretized foil and cavity surfaces in a partially-cavitating condition.

4.2 Approximation of integral equation

Assume that the strengths of sources and normal dipoles are constant on each panel, that is

$$\mu(\xi)=\mu_j, \text{ on panel } j, j=1,\cdots,N^D+1 \tag{27}$$

$$q(\xi)=q_k, \text{ on panel } k, k=1,\cdots,N^S \tag{28}$$

where N^D+1 and N^S denote the number of panels on which normal dipoles and sources are distributed, respectively. Since the source panels always coincide with the dipole panels, the total number of panels to represent the foil-cavity system will be N^D. We will not count the dipole for the wake sheet surface just for convenience, since it is always represented as a function of the other dipole strengths.

The control point on the foil-cavity surface, $\underline{x}^D$, where the boundary conditions are to be satisfied, is positioned at the center of each element, such that

$$\underline{x}_i^D=\frac{1}{2}(\underline{x}_i+\underline{x}_{i+1}),\ i=1,\cdots,N^D \tag{29}$$

where $\underline{x}_i$ may either be the panel boundary coordinate of the hydrofoil, $\underline{x}^B=(x^B, y^B)$, or that of the cavity, $\underline{x}^C=(x^C, y^D)$.

Distributing the normal dipoles on the surfaces of both hydrofoil and cavity and the sources on the cavity surface, we can express the total velocity potential at the ith control point as follows :

$$\Phi_i^- = 0 = \underline{U}_\infty \cdot \underline{x}_i^D + \sum_{j=1}^{ND} \frac{\mu_j}{2\pi}\beta_{ij} + \sum_{k=1}^{NS} \frac{q_k}{2\pi}\alpha_{ik} + \frac{\mu_w}{2\pi}\beta_{iw} \tag{30}$$

where

$$\beta_{ij}=\begin{cases}\pi & , \text{if } i=j\\ \int_{C_j}\frac{\partial}{\partial n_j} log\ R(\underline{x}_i;\underline{\xi}_j)\,dS & , \text{if } i\neq j\end{cases}$$

$$\alpha_{ik}=\int_{C_k} log\ R(\underline{x}_i;\underline{\xi}_k)\,dS$$

$$\beta_{iw}=\int_{S_w}\frac{\partial}{\partial n_w} log\ R(\underline{x}_i;\underline{\xi}_w)\,dS$$

where the subscripts i and j denote the ith control point and the jth singularity point, respectively, and the subscript w represents the wake surface.

An approximate expression for the Kutta condition (6) is obtained, following the Morino's condition (20), as

$$\mu_w=-(\Delta\Phi)_w-\Phi_1-\Phi_{N^D}=-(\mu_1-\mu_{N^D}) \tag{31}$$

where the subscripts 1 and N^D link the values to the lower and upper surface panels, respectively, adjacent to the trailing edge.

Following (21) which is derived from the dynamic boundary condition, the total velocity potential at the control point of the jth source panel along the cavity surface in the streamwise direction can be expressed as follows :

$$\Phi_i^u=\Phi_{i,dp}^u+|\underline{V}_i|\sum_{k=1}^{j}\Delta s_k^u \tag{32}$$

where $\Phi_{i,dp}^u$ denotes the total velocity potential on the cavity detachment points at the leading edge of the hydrofoil, and Δs_k^u denotes the length of the kth source panel along the upper cavity surface.

Since $\Phi_i=\Phi_i-\mu_i=-\mu_i=-\mu_w$, the above relation becomes

$$\mu_i^u=\mu_{i,dp}^u-|\underline{V}_i|\,l_e \tag{33}$$

where

$$l_e=\sum_{k=1}^{i}\Delta s_k$$

Equation (33) shows that strengths of normal dipoles on the cavity surface can be expressed as a linear function of the dipole strengths at the cavity detachment point and the tangential speed on the cavity surface, $|\underline{V}_i|$; that is, there is no unknown dipole strength on the cavity surface.

Upon discretization, the cavity closure con-

dition (25) for the partially-cavitating flow will be recast as

$$\sum_{k=1}^{N^S} q_k \Delta s_k = 0 \tag{34}$$

The total number of unknowns is N^D+1, which consists of (N^D+N^S) unknown dipoles, (N^S) sources and $|\underline{V}_c|$. To determine the unknowns we need the same number of equations, which may be formed by applying (30) to N^D control points defined in (29) and by applying the closure condition (34).

4.3 Discussion on solution procedure

Upon formation of the linear system of algebraic equations, we may need to check the well-posedness of the present numerical formulation. Unlike the solution technique for the problem of the non-cavitating flow with a proven record, it is likely that the present method may be affected by the presence of the sources, which will influence the diagonal element of the coefficient matrix through the weak self-induced potential values a_{ii} in (30). The value of a_{ii} is determined by $\delta_s(log\ \delta_s/2-1)$ where δ_s is the panel size. It is small but clearly nonzero. According to a criterion in Press et al[12], the inverse of the condition number, for a typical hydrofoil with 6 percent thickness-chord ratio with $N^D=100$ and $N^S=25$, is 10^{-4}, which is small but gives still a large room to the double precision machine limit of 10^{-12}, whereas the noncavitating fully wetted problem gives the condition number of 10^{-3} for the similar case with $N^D=100$(see, p.54 of Press et al[12] for definition of the condition number and details on the matrix solver *SVDCMP* used for the test.).

After determining the strengths of sources and normal dipoles, through the solution of the simultaneous equations, the cavity thickness may be computed by integrating the source strengths in accordance with (24) and by using (23). In this paper, only the vertical coordinate of the cavity surface is evaluated. Once the cavity surface is found for the present step, the sources and normal dipoles are to be relocated on the newly obtained cavity surface, and then the process is repeated until a sufficient convergence is achieved. Upon convergence, the strength of the sources vanishes and the converged cavity shape is obtained.

For the first iteration, it is necessary to assume the initial cavity geometry. A simple quadratic cavity shape with maximum thickness to be equal to the foil thickness was assumed. The initial approximation of the cavity geometry is however found irrelevant to the final solution as long as the shape is represented by a smooth simple curve. Based on this numerical experiments, we conclude that the solution is convergent to a true solution regardless of the initial guess of the cavity shape. For most of the engineering calculations, a few iterations is found sufficient, but for most of sample calculations, the number of iterations, N^{iter}, is set to 10.

Once we get the dipole distribution, then we can compute the tangential speed $|\underline{V}_t|$ by differentiating the total potential values (which is negative of the dipole strength) along the foil-cavity surface. We use a simple quadratic differentiation formula to take derivatives. Equation (10) is then used to compute the pressure coefficient, from which the lift, drag and moment coefficients are obtained by evaluating (13) through (15), and the cavity volume is obtained by (16). The cavitation number, σ or σ_{comp}, is computed by substituting into (11) the tangential speed on the cavity surface, $|\underline{V}_c|$, which is obtained directly by solving the simultaneous equation.

5. Numerical calculations and discussions

5.1 Convergence test

The first step to implement the numerical pro-

cedure is to show the convergence characteristics of the discretization.

An *NACA* 16-006 hydrofoil section, which was used by Uhlman[5], is chosen for both convergence test and comparison. The computations are made for the foil at an angle of attack $\alpha=4$ deg and with a cavity extent of 50 percent of the chord length.

Fig. 4 shows the influence of panel numbers upon the computed cavitation number, σ, for various number of panels, $N^D(=48, 100, 148, 200)$, while looking for the final converged cavity profile through an iterative procedure, together with those of Uhlman. As the number of panels and iterations is increased, the two methods are shown to converge to a common value. The computed cavitation index predicted by the present theory, $\sigma_{comp}=0.885$, is 1.0 percent higher than that of Uhlman, $\sigma_{comp}=0.874$.

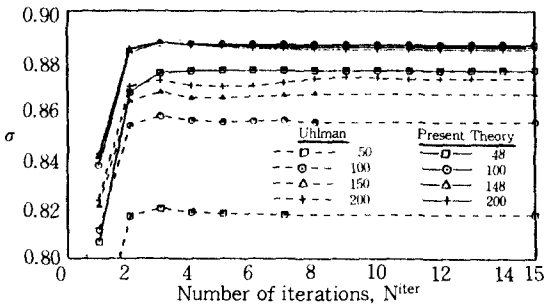

Fig. 4 Convergence, σ versus number of iterations (NACA 16-006 section, $\alpha=4$ deg, $l/c=0.50$, for $N^D=48$, 100, 148, 200). Comparison with Uhlman

Although the present formulation based on the potential function is different from that of Uhlman based on the velocity function, the final results are very close to each other. The present approach, however, proved superior to Uhlman's by showing the convergence error to be less than 0.2 percent when the panel numbers are varied from 100 to 200. For engineering purposes, it may be seen sufficient to iterate twice with $N^D=48$.

To compare with other theories and experiments, all the subsequent computations are made with $N^D=100$ and $N^{iter}=5$ unless otherwise stated explicitly.

Fig. 5 shows the convergence behavior of the cavity volume, obtained with the same condition as in Fig. 4.

The converged cavity shape is illustrated in Fig. 6. The computed cavity shapes from the second and fifth iterations are so close that the fast convergence of the cavitation index and volume is readily expected.

In Fig. 7, the pressure distributions on the foil and cavity surfaces are compared for two different panel numbers. Except at the cavity trailing end, where the theory is not expected to be so accurate, the pressure distributions show a good convergence.

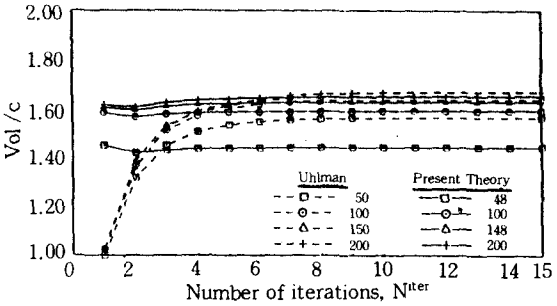

Fig. 5 Convergence, Vol/c^3 versus number of iterations(NACA 16-006 section, $\alpha=4$ deg, $l/c=0.50$, for $N^D=48$, 100, 148, 200). Comparison with Uhlman

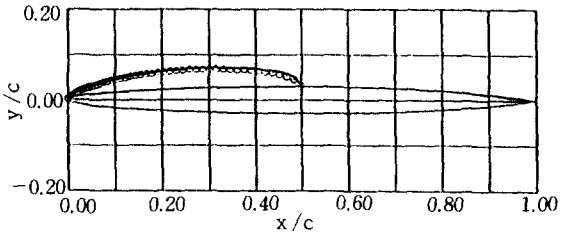

Fig. 6 Cavity shape after 5-th iteraction(- -) and 2-nd iteration(⊙) for cavitating NACA 16-006 section with $l/c=0.50$ at $\alpha=4$ deg

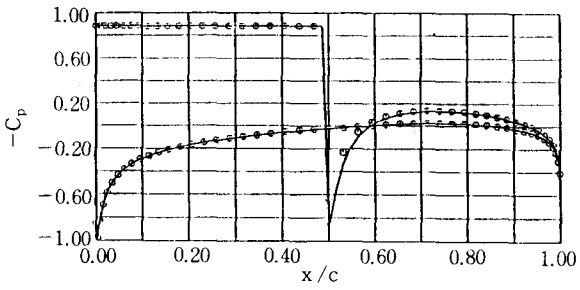

Fig. 7 Pressure distribution, NACA 16-006 section, $\alpha=4$ deg, $l/c=0.50$, for $N^D=200$(- -) and $N^D=100$(⊙)

5.2 Influence of blade thickness

It has been reported by Uhlman [5] that, for the same α/σ when $l_{cav}/c < 0.75$, the thicker blade section produces the shorter cavity. This result, contrary to the prediction by the linear theory, raised the need for nonlinear analysis.

The study on the thickness effects is repeated here with the same NACA 16 hydrofoil as in Uhlman in Fig. 8. The prediction by Uhlman is confirmed by the present theory, which shows, however, a more pronounced thickness effect than Uhlman.

5.3 Comparison with experiment

Experimental data on the observation of cavity length are so rare that the experimental verification of a theory can not be made easily, especially for the hydrofoil sections with a round leading edge.

An experiment by Meijer [13] for a symmetric section with a biconvex profile provides therefore very valuable information and a guide to a new theory.

Meijer's experimental data for a 4 percent biconvex foil are compared with the present theory in Fig. 9, where the relation of the cavity length versus α/σ is plotted. This experiment was originally carried out to verify the theory of Geurst [14] and was adopted by Uhlman to check his linear and nonlinear theories.

It may be concluded that both the

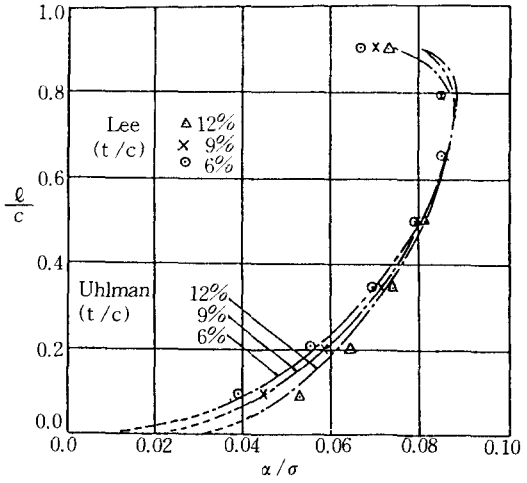

Fig. 8 l/c versus α/σ, NACA 16 series sections, $\alpha=4$ deg. Comparison with Uhlman

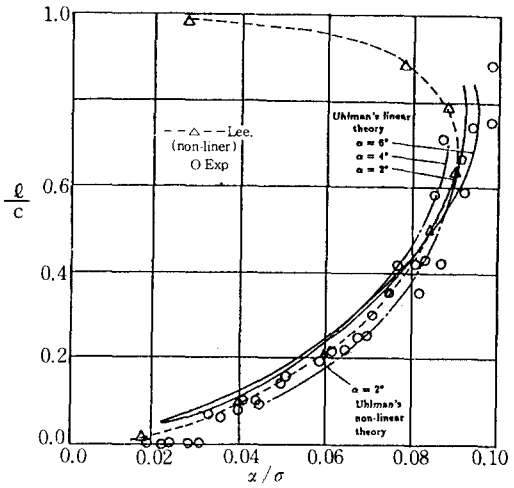

Fig. 9 Comparison with Meijer's experimental data for a 4 percent biconvex foil. Linear and nonlinear theories of Uhlman are added for comparison

nonlinear theories of Uhlman and of the present paper give good correlation with the experiment in the range of $l_{cav}/c < 0.75$.

6. Conclusions

A potential-based surface panel method is

formulated for the solution of partially-cavitating flow problem about a two-dimensional hydrofoil. The method employs the normal dipole and source distributions on the foil and cavity surfaces. It is shown that the source plays an important role in positioning the cavity surface through an iterative process. The cavity closure condition, which forces the net strength of the sources to vanish, is found very effective in generating the closed cavity shape.

Extensive convergence tests are carried out to show the influence of discretization scheme and the iterative procedure. The numerical method shows extremely fast and stable convergence characteristics.

It is shown that the thicker blade section produces the shorter cavity. This result is contrary to the linear prediction.

In the region of small angle of attack, the prediction shows an excellent comparison with the Geurst's linear theory.

For a biconvex hydrofoil, the theory shows a good correlation with the experimental results by Meijer.

7. Acknowledgements

Financial support from Korea Science and Engineering Foundation and Hyundai Maritime Research Institute is greatly acknowledged.

References

[1] Lee, C.-S., "Prediction of Steady and Unsteady Performance of Marine Propellers with or without Cavitation by Numerical Lifting Surface Theory", Ph.D. Thesis, Department of Ocean Engineering, M.I.T., Cambridge, Mass., 1979.

[2] Lee, J.-T., "A Potential-based Panel Method for the Analysis of Marine Propellers in Steady flow", Ph.D. Thesis, Department of Ocean Engineering, M.I.T., Cambridge, Mass., 1987.

[3] Yang, C. I. & Jessup, S. D., "Benchmark Analysis of a Series of Propellers with a Panel Method", *SNAME* Propelier '88 Symp., Virginia Beach, VA, 1988, pp. 17/1-10.

[4] Hess, J. L., & Valarezo, W. O., "Calculation of Steady Flow about Propellers by Means of a Surface Panel Method", The 23rd Aerospace Science Meeting, *AIAA*, Reno, Nevada, Jan. 1985.

[5] Uhlman, J. S., "The Surface Singularity Method Applied to Partially Cavitating Hydrofoils", *J. of Ship Research*, Vol. 31, No. 2, June 1987, pp. 107−124.

[6] Wu, T. Y., "Inviscid Cavity and Wake Flows", *Basic Developments in Fluid Dynamics*, Vol. 2, Academic Press Inc., New York, 1968.

[7] Wu, T. Y., "Cavity and Wake Flows", *Annual Review of Fluid Mechanics*, Vol. 4, 1972, pp. 243−284.

[8] Lamb, H., "Hydrodynamics", Dover Publications, N.Y., 1945, pp. 59−60.

[9] Moran, J., "An Introduction to the Theoretical and Computational Aerodynamics", *John Wiley & Sons*, 1984, pp. 118−123.

[10] Breslin, J.P., Van Houten, R.J., Kerwin, J.E. & Johnsson, C.A., "Theoretical and Experimental Propeller-Induced Hull Pressures Arising from Intermittent Blade Cavitation, Loading, and Thickness", *SNAME Trans.* Vol. 90, 1982, pp. 111−151.

[11] Morino, L. and Kuo, C.-C., "Subsonic Potential Aerodynamic for Complex Configurations: a General Theory", *AIAA J.*, Vol. 12, No. 2, 1974, pp. 191−197.

[12] Press, W.H., Flannery, B.P., Teukolsky, S.A. and Vetterling, W.T., "*Numerical Recipes: The Art of Scientific Computing*", Cambridge Univ. Press, 1986, p. 54.

[13] Meijer, M.C., "Some Experiments on Partly Cavitating Hydrofoils", *Internationl Shipbuilding Progress*, Vol. 6, No. 60, Aug. 1959.

[14] Geurst, J.A., "Linearized Theory of Two Dimensional, Cavitating, Lifting Flow", Thesis, Delft Technical Institute, The Netherlands, 1961.